BIOCHEMISTRY
including biophysical chemistry & molecular biology

Article

pubs.acs.org/biochemistry

Phosphatidylcholine Attenuates Aggregation of Nonsteroidal Anti-Inflammatory Drugs with Bile Acid

Priyanka Prakash and Alemayehu A. Gorfe*

Department of Integrative Biology and Pharmacology, University of Texas at Houston, 6431 Fannin Street, Houston, Texas 77030, United States

Supporting Information

ABSTRACT: Prolonged usage of nonsteroidal anti-inflammatory drugs (NSAIDs) causes gastrointestinal injury. Bile acids and phospholipids have been shown to exasperate and attenuate NSAIDs' toxicity, respectively. However, the molecular mechanisms underlying these effects remain undetermined. We have investigated the molecular interactions in various mixtures of indomethacin (Indo), a commonly used NSAID, and cholic acid (CA), a bile acid, in the presence and absence of palmitoyloleylphosphatidylcholine (POPC) lipids. We found that CA and Indo spontaneously form mixed micelles, with the hydrophobic face of CA and hydrophobic region of Indo forming the core. Increasing the Indo concentration resulted in more stable and larger aggregates that contain a progressively larger number of Indo molecules. More dynamic aggregates with a maximum size of 15 were obtained when the relative concentration of CA was higher. The mixture of CA, Indo, and POPC also led to ternary mixed micelles in which CA and Indo distribute almost uniformly on the surface such that intra-CA, intra-Indo, and CA/Indo interactions are minimized. A number of previous reports have shown that Indo perforates the cell membrane in the presence of bile acids (e.g., Petruzzelli et al., (2006) *Dig. Dis. Sci.*, *51*, 766−774). We propose that this may be related to the stable, highly charged, large CA/Indo binary micelles observed in our simulations. Similarly, the diminished ability of the CA/Indo mixture to aggregate in the presence of POPC may partly explain the lower toxicity of PC-conjugated NSAIDs.

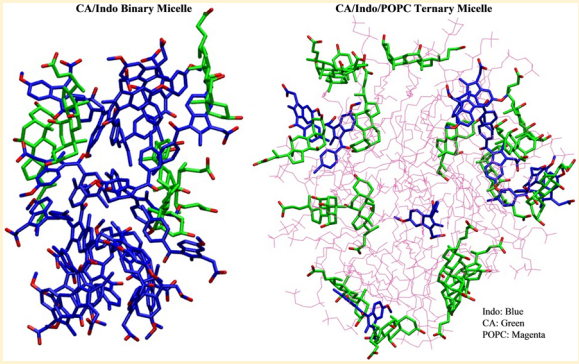

It is well established that chronic use of nonsteroidal anti-inflammatory drugs (NSAIDs) causes gastrointestinal (GI) injury and bleeding.[1−9] The therapeutic action of NSAIDs involves the inhibition of cyclooxygenase.[10,11] However, numerous studies have shown that NSAID-induced GI injury is independent of cyclooxygenase activity[12−14] and that bile salts increase the toxicity of NSAIDs to the lower GI tract.[3−6] The latter is especially true for those NSAIDs that undergo enterohepatic circulation, such as indomethacin (Indo).[15,16] These observations suggest that bile salts either enhance the intrinsic cytotoxicity of NSAIDs or interact with them to form membrane-damaging molecular species.[3,17] In contrast, phosphatidylcholine (PC) lipids attenuate NSAID cytotoxicity via an unknown mechanism, possibly by preventing direct contact between the drugs and intestinal membrane.[18−24] Despite the intriguing implication of these findings for physiology and biotechnology, it remains unknown how bile salts and NSAIDs might interact at the molecular level or how PC-conjugation of NSAIDs reduces injury.

Bile acids (BA) are released from the gallbladder into the small intestine where they serve as a digestive surfactant to facilitate the absorption of nutrients. The facially amphipathic monomeric BA (Figure 1) as well as pure-BA micelles are believed to have an adverse effect on the GI mucosa.[25,26] Under normal physiologic conditions, however, bile salts exist as mixed micelles with PCs and therefore are noninjurious.[25−28]

To our knowledge there is no data on the molecular mechanism underlying the assembly of a BA, PC, and NSAID ternary mixture. However, considerable effort has been made toward understanding the driving forces and molecular interactions responsible for BA self-assembly.[29−33] It was found that the concentration-dependent aggregation of BA leads to the formation of molecular structures whose morphologies markedly differ from aggregates of conventional surfactants.[29,31−35] In addition, several groups have investigated the aggregation behavior of BA and PC mixtures and found that the aggregates are loosely bound and can assemble or disassemble easily.[36−43] Moreover, two types of shapes have been proposed to characterize BA-PC aggregates: stacked-disk and radial-shell.[29,31−37] Previously, we used fully atomistic molecular dynamics (MD) simulations to investigate the self-assembly of one of the most common bile salts, cholic acid (CA),[33] as well as the aggregation of CA with ibuprofen (Ibu) in the absence and presence of a preformed dodecylphosphocholine (DPC) micelle.[37] We found that in each case CA self-assembled into micelles of mean size 5 to 6,[33,37] in close agreement with experimental results.[44] Moreover, CA and Ibu

Received: June 7, 2013
Revised: August 23, 2013
Published: September 25, 2013

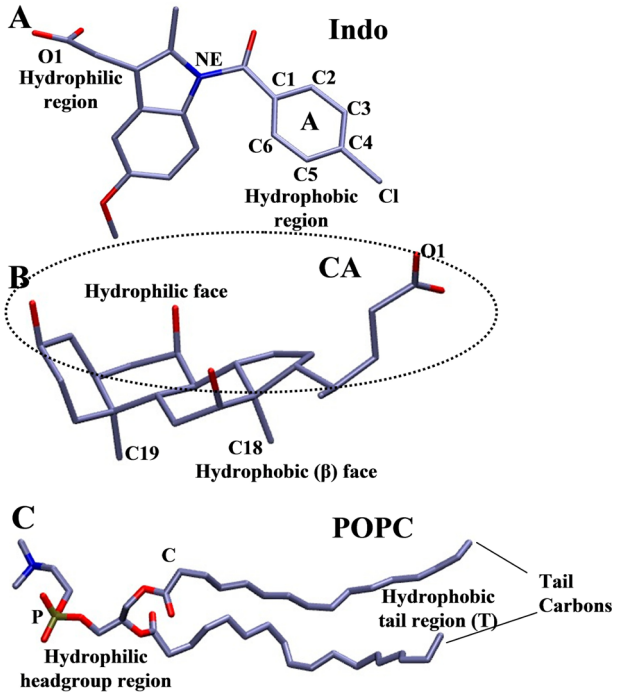

Figure 1. Structure of three chemical species whose mixture was simulated in this study. (A) Indomethacin (Indo). (B) Cholic acid (CA). (C) Palmitoyloleylphosphatidylcholine (POPC). The hydrophilic face of CA involves its three hydroxyl and the two carboxyl oxygen atoms.

formed mixed micelles whose size became significantly smaller in the presence of the preformed DPC micelle.[37]

A major aim of this work was to test if another NSAID, Indo, interacts with and alters the micellar organization of CA and/or CA/PC mixtures. In contrast to our previous work where we used a preformed DPC micelle as a PC mimic, here we use palmitoyloleylphosphatidylcholine(POPC), a regular double-tailed phospholipid that normally forms bilayer. Using a number of all atom explicit solvent MD simulations of total length greater than a microsecond, we characterized the molecular interactions, stability, and morphology of the CA/Indo binary as well as CA/Indo/POPC ternary micelles. Although the overall behavior of the CA/Indo micelles was found to be similar to that of CA/Ibu micelles,[37] we found that POPC significantly attenuates the ability of CA and Indo to form (potentially cytotoxic) binary micelles.

1. METHODS

1.1. System Setup and MD Simulations. We carried out nine independent (MD) simulations on different mixtures of CA, Indo, and POPC, including four CA/Indo mixtures, three CA/Indo/POPC mixtures, a CA/POPC mixture, and a pure-Indo simulation (Table 1). The starting configuration and parameters for Indo and CA were prepared using the CHARMM general force field (CGenff) for small ligands.[45] The CHARMM27 force field[46] was used to model POPC, water, and ions. The 3D structures of CA, Indo, and POPC are shown in Figure 1.

The simulation setup was similar to that described before.[33,37] Briefly, for the pure-Indo and the binary and ternary mixtures, the solute molecules (i.e., CA, Indo, and POPC) were randomly placed in a cubic box of length 100 Å containing TIP3 waters. The net charge of the system was neutralized by adding Na^+ ions in equal number to the total number of the negatively charged CA and Indo molecules. For faster equilibration, the Na^+ ions were distributed randomly in a sphere of radius 3−5 Å around the center of the carboxyl oxygen atoms of CA and Indo. Each system was energy-minimized by the steepest descent method for 100 000 steps and equilibrated as described previously.[33,37] The simulations were carried out using the NAMD program[47] at 310 K and 1 atm. Langevin dynamics with a damping coefficient of 10 ps^{-1} was used to maintain constant temperature, and the Langevin-piston method was used to maintain constant pressure. Periodic boundary condition with particle mesh Ewald[48] was used with a 12 Å cutoff for nonbonded interactions and 14 Å for nonbonded list update. Production runs lasted 80 ns for pure-Indo and CA/POPC mixtures, 100 ns for all other binary mixtures, and 200 ns for the ternary mixtures. Unless stated otherwise, the best-equilibrated last 30 ns for the pure-Indo and binary mixtures and the last 50 ns portion for the ternary mixture trajectories was used for the analysis of equilibrium quantities such as micelle size and morphology.

1.2. Data Analysis. We monitored the time evolution and stability of the aggregates during the simulations by the number-averaged (N_N) aggregation number (Figure S1). The weight-averaged aggregation number (N_W) was also calculated to obtain the polydispersity index ($\langle N_W\rangle/\langle N_N\rangle$). N_N and N_W were calculated as described before,[33] and micelles were defined on the basis of a simple distance-based criterion involving the C18 carbon atom of CA (CA:C18) and the nitrogen atom of Indo (Indo:NE). (For atom numbering, see Figure 1.) Thus, if the distance between the nitrogen atom of an Indo molecule and the C18 atom of a CA molecule is less than 10 Å, then these two molecules were defined as being part of the same mixed micelle. Likewise, if the distance between a nitrogen

Table 1. Summary of the CA/Indo and CA/Indo/POPC Simulations[a]

simulation	CA/Indo	[POPC] (mM)	[CA] (mM)	[Indo] (mM)	time (ns)	N_N	polydispersity index
$S_{1:0.5}$	1:0.5		49.8	24.9	100	5.2 ± 0.5	1.2
$S_{1:1}$	1:1		49.8	49.8	100	9.3 ± 1.1	1.3
$S_{1:2}$	1:2		49.8	99.6	100	8.6 ± 0.6	1.3
$S_{1:4}$	1:4		49.8	199.2	100	14.2 ± 0.8	1.2
$S^P{}_{1:1}$	1:1	99.6	24.9	24.9	200	2.4 ± 0.3	1.1
$S^{P'}{}_{1:1}$	1:1	99.6	49.8	49.8	200	3.0 ± 0.3	1.2
$S^P{}_{1:0.5}$	1:0.5	99.6	99.6	49.8	200	4.4 ± 0.4	1.6

[a]Reference simulations (not listed here) of pure-Indo and a CA/POPC mixture were run for 80 ns each. For S^P simulations, only N_N values of CA/Indo aggregates in the ternary mixture are reported.

dx.doi.org/10.1021/bi400723r | Biochemistry 2013, 52, 7461−7469

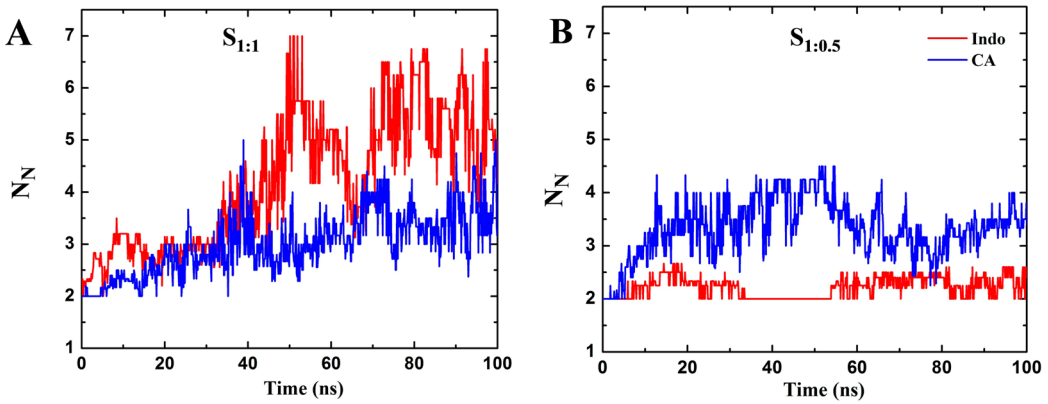

Figure 2. Aggregation profile of CA and Indo in CA/Indo mixed micelles. Number-averaged aggregation number (N_N) of pure-CA (blue) and pure-Indo (red) micelles in CA/Indo binary mixtures from simulations (A) $S_{1:1}$ and (B) $S_{1:0.5}$.

atom of one Indo (or C18 of CA) molecule is within 10 Å of the nitrogen atom of another Indo (or C18 of CA) molecule, then that Indo (or CA) molecule was defined as belonging to a pure-Indo (or pure-CA) aggregate. CA and Indo molecules that did not satisfy this condition were defined as monomers. We defined a CA/Indo/POPC ternary micelle based on the condition that if POPC:C, Indo:NE, and CA:C18 are within 12 Å of each other, then they belong to the same micelle. We refer to aggregates of two or more types of reactants as mixed micelles and those made up of only CA or only Indo as pure-CA and pure-Indo micelles, respectively. The terms aggregate and mixed micelle are used interchangeably throughout this paper. An aggregate of size *n* thus represents a micelle of size *n*.

2. RESULTS AND DISCUSSION

We first discuss the assembly of the mixed micelles during the simulations followed by their structural and thermodynamic property using the best-equilibration portion of the trajectories.

2.1. Spontaneous Formation of CA/Indo and CA/Indo/POPC Mixed Micelles. *2.1.1. Various Mixtures of CA and Indo Lead to Polydisperse Mixed Micelles.* We have simulated CA and Indo mixtures at four different molar ratios, where the concentration of CA was fixed at 49.8 mM (above its critical micellar concentration (CMC) of 25−30 mM)[37] and that of Indo was varied between 25 and 200 mM (simulations $S_{1:0.5}$, $S_{1:1}$, $S_{1:2}$, and $S_{1:4}$; Table1). Note that in order to achieve aggregate formation within a reasonable MD time scale we had to use concentrations that are much higher than the physiological ones, assuming that the process of assembly and the morphology of the final aggregates would be not very sensitive to changes in concentrations. Indeed, each of the four CA/Indo simulations yielded multiple CA/Indo mixed micelles with similar overall structure, as illustrated in Figure S2 using a snapshot of a typical CA/Indo system at the 100 ns time point of an MD run. The process of aggregation is shown in Figure S1 based on the time evolution of the number-averaged aggregation number (N_N) in each simulation. From the profiles of N_N, one can see that aggregation was complete within about 30 ns in each of the simulations except for $S_{1:1}$, which took about 70 ns to stabilize. These time scales are on the same order of magnitude as the aggregation time scales of pure-Indo or CA in water, which spontaneously self-assembled within ∼20 (Figure S3) and ∼25 ns,[33] respectively. For consistency, we used only the last 30 ns of the data from the current simulations for the subsequent analysis of thermodynamic and structural quantities (Results and Discussion, sections 2.2.1 and 2.2.2).

To evaluate the relative role of CA and Indo in the aggregation process, we monitored the time evolution of N_N of pure-CA and pure-Indo aggregates in the CA/Indo binary mixtures (Figure 2A,B). Indo aggregated faster than CA when its fraction was either higher or equivalent to CA (Figure 2A). For example, after about 10 ns of simulation $S_{1:1}$, N_N of pure-Indo was ∼3.5, whereas that of pure-CA was ∼2.5 (Figure 2A); this difference was maintained and even increased in the rest of the simulation time. To our knowledge, the CMC of Indo is not known, but this result appears to suggest that it may be lower than the CMC of CA. Although Indo aggregates first in the 1:1 CA/Indo mixture, a higher CA concentration (ca. simulation $S_{1:0.5}$) resulted in a faster aggregation of CA (Figure 2B). Overall, therefore, the reactant with the higher relative concentration aggregates faster, although Indo aggregates slightly faster than CA when it is both in the pure phase and in an equimolar mixture with CA. This result predicts that under physiologic conditions CA/Indo assembly may also proceed via random collision so that the species existing at a higher proportion dictates the kinetics.

2.1.2. Spontaneous Micellization of CA/POPC and CA/Indo/POPC Mixtures. Experiments have shown that bile salts form mixed micelles with egg-yolk PC and DPPC.[39,42,43] Therefore, before delving into the CA/Indo/POPC mixtures, we simulated a 2:1 (mol %) CA/POPC mixture. We observed a fast spontaneous aggregation of CA and POPC into a binary micelle that has a radial-shell shape, consistent with previous simulation results on a similar CA/POPC mixture[36] as well as a CA/DPC mixture.[33] We then carried out three simulations of CA, Indo, and POPC mixtures in which the molar ratio of CA and Indo was varied but the concentration of POPC was fixed at 99.6 mM (Table 1). The goal was to see if PC alters the aggregation behavior of Indo with CA or if Indo modulates the aggregation of CA and POPC. Each of the three mixtures that we tested led to CA/Indo/POPC ternary micelles (Figure S4). When compared with the relatively fast aggregation observed in the binary mixtures, the formation of ternary micelles was a slower process that took between 70 and 150 ns, which is to be expected. Once formed, however, the ternary micelles were stable for the rest of the simulation time. Analysis was therefore performed on the last 50 ns portion of each trajectory unless stated otherwise.

In the CA/POPC mixture, pure-CA aggregates were formed with a dominant aggregate of size 5 (Figure S5), in agreement

dx.doi.org/10.1021/bi400723r | *Biochemistry* 2013, 52, 7461−7469

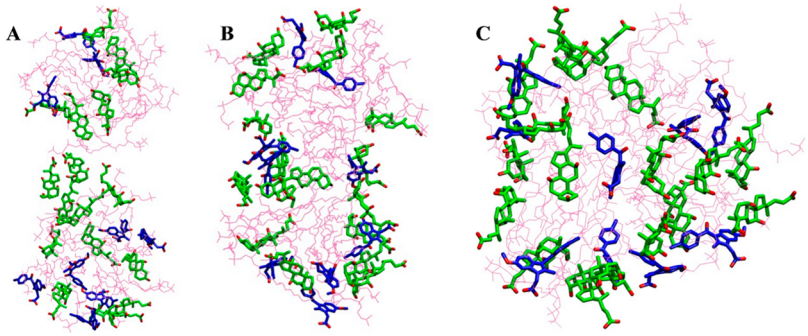

Figure 3. Formation of CA/Indo/POPC ternary micelles. (A) Prefusion, where two smaller ternary micelles are close to each other but did not fuse. (B) Postfusion, where two micelles fused into a single micelle but did not adopt the final morphology. (C) Final aggregate formed after reorganization of the postfusion intermediate into a more spherical micelle. One of the largest aggregates (aggregate size 54 from simulation $S^{P}_{1:0.5}$) was used for illustration. POPC, CA, and Indo are shown in magenta, green, and blue, respectively. Oxygen atoms are shown in red.

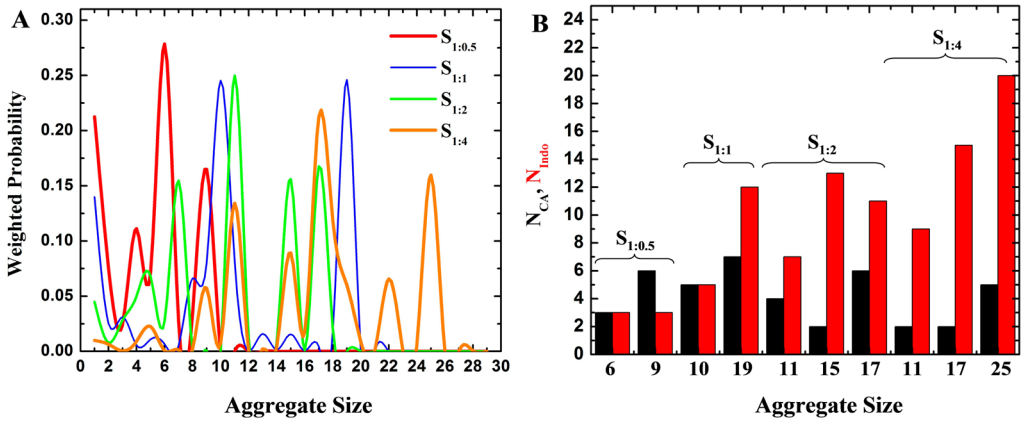

Figure 4. Predominant aggregates in CA/Indo binary mixtures. (A) Weighted probability distribution of CA/Indo aggregates of size *n* and (B) average number of CA (N_{CA}, black) and Indo (N_{Indo}, red) in the most stable micelles (>75% occurrence).

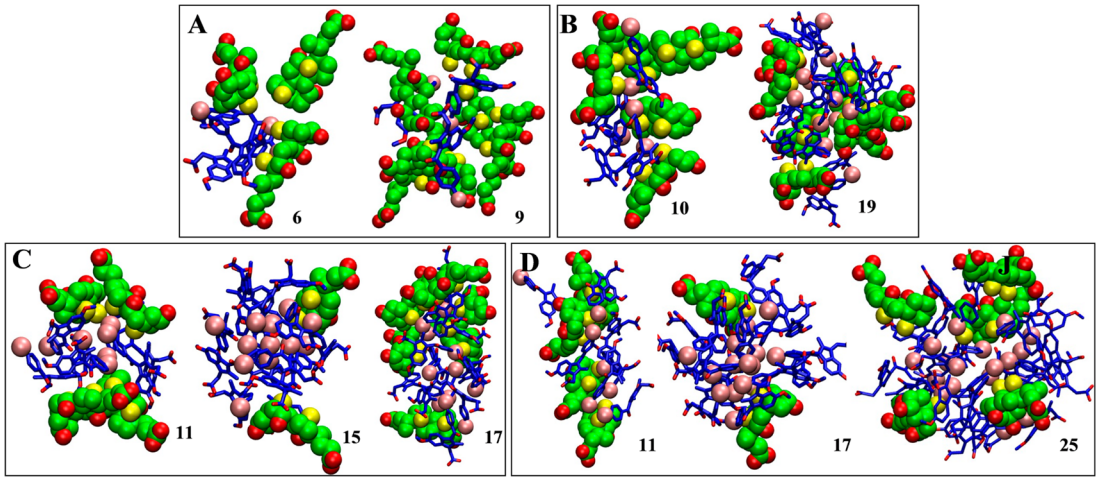

Figure 5. Last snapshot of the predominant CA/Indo aggregates from different simulations. The size of the micelles from simulations (A) $S_{1:0.5}$, (B) $S_{1:1}$, (C) $S_{1:2}$, and (D) $S_{1:4}$ are indicated. The green vdW spheres represent CA, and the blue licorice represents Indo. The C18 and C19 methyl carbons of CA and the Cl atom of Indo are shown in yellow and pink spheres, respectively, whereas all oxygen atoms are in red (refer to Figure 1 for atom numbering).

with our previous observations with a preformed DPC micelle.[33] However, in contrast to both the CA/Indo or CA/PC simulations, no pure-CA or pure-Indo micelle was observed in the ternary mixture. In other words, every CA and Indo molecule was either part of a CA/Indo or CA/Indo/POPC micelle or remained a monomer. However, it is important to note that the CA/Indo aggregates in the ternary mixture are the subset of the ternary mixed micelle (i.e., almost all of the CA and Indo molecules were part of a ternary micelle). In each simulation, approximately spherical ternary micelles were formed through the fusion and subsequent reorganization of smaller micelles (Figure 3), with the final complex looking similar to that obtained by the adsorption of CA and Ibu on a preformed DPC micelle. That the random mixing of CA, Indo,

dx.doi.org/10.1021/bi400723r | *Biochemistry* 2013, 52, 7461−7469

and POPC led to similar results to that obtained with a preformed DPC micelle suggests that complexation may be a universal behavior of NSAID/BA/PC mixtures.

2.2. Equilibrium Properties of CA/Indo and CA/Indo/POPC Micelles. *2.2.1. CA/Indo Mixed Micelles Are Larger than Pure-CA or Pure-Indo Micelles.* The ensemble averaged N_N for pure-Indo (7.4 ± 0.3, see Figure S3) was higher than that of pure-CA (4.5 ± 0.38, ref 33). Importantly, both of these values are significantly smaller than the N_N of the mixed micelles from simulation $S_{1:1}$ (9.3 ± 1.1, see Table 1). Note that the total solute concentration was similar in the pure-Indo (3.6g/dL), pure-CA (4.1g/dL) and $S_{1:1}$ (4.1g/dL) simulations. Therefore, mixing the two leads to larger micelles than those from either CA or Indo in isolation. Moreover, the overall increase of N_N with the mole fraction of Indo (Table 1) suggests that larger aggregates are more common at a higher Indo concentration, in agreement with our previous finding for CA and Ibu mixtures.[37] In contrast, size heterogeneity is not a function of concentration, as can be judged from the very similar polydispersity indices at different CA/Indo molar ratios (Table 1).

Focusing on the CA/Indo micelles whose probability of occurrence was more than 10% (as seen from the cluster size distribution calculated as described before[33,37] (Figure 4)), we find that aggregates of size 6 and 9 ($S_{1:0.5}$), 10 and 19 ($S_{1:1}$), 7, 11, 15, and 17 ($S_{1:2}$), and 11, 17, and 25 ($S_{1:4}$) are the predominant species (Figures 4A and 5). Examination of the average number of CA (N_{CA}) and Indo (N_{Indo}) within these predominant CA/Indo micelles indicated that the species present at higher faction is more abundant in the mixed micelles (Figure 4B). That is, $N_{CA} \geq N_{Indo}$ in $S_{1:0.5}$, whereas in all others $N_{Indo} \gg N_{CA}$. Note, however, that N_{CA} is always less than 7, whereas N_{Indo} can be as high as 20 (Figure 4B); even when the CA fraction was made 4-fold higher, the total aggregation size remained below 15 (Figure S6). Previous studies have shown that, even at CA concentrations as large as 300 mM, the aggregation number of CA remains smaller than 12.[33,35] This suggests a steric limit to the total number of CA that can pack together. Instead, primary CA micelles tend to form larger secondary micelles, a phenomenon proposed by Carey and Small[31] (Figure S6). Indo can form larger micelles in the pure phase as well as in the presence of CA. This can be understood from the fact that Indo's structure and shape is intermediate between the planarly amphipathic CA and linearly amphipathic surfactants, such as lipids.

To characterize the shape and make up of the CA/Indo mixed micelles in detail, we focused only on those micelles that were stable for at least 75% of the time in the last 30 ns of each simulation (Table 2). Visual inspection of these micelles suggested, once again, that larger clusters contain more Indo molecules than CA (Figure 5). More quantitatively, the average CA/Indo ratio in mixed micelles of size 11 and 17 was 3:8 and 4:14, respectively. The morphology of these micelles was evaluated on the basis of their principal moments of inertia, I_1, I_2, and I_3, calculated as described previously.[33,37] The resulting I_1/I_2 versus I_2/I_3 bivariate distributions show that micelles of size 11 adopt an oblate-ellipsoidal shape ($I_1/I_2 \approx 0.4$ and $I_2/I_3 \approx 0.9$), whereas those of size 17 have a cylindrical or disk-like shape (Figure S7). Partay et al.[35] found that the preferred shape of pure-CA micelles was oblate-ellipsoidal. At higher concentration, Indo was thus able to alter the morphology of pure-CA micelles. Moreover, both the size and overall shape of the stable CA/Indo micelles in the current study differ from those preferred by CA-Ibu micelles,[37] suggesting that different NSAIDs may form micelles of different size and composition with potentially different biochemical properties.

Table 2. Stability of the Most Populated Aggregates in the Last 30 ns of Simulations $S_{1:0.5}$ through $S_{1:4}$

simulation	aggregate size	occurrence (%)
$S_{1:0.5}$	6	93.6
$S_{1:0.5}$	9	77.0
$S_{1:1}$	10	83.1
$S_{1:1}$	19	77.7
$S_{1:2}$	11	98.5
$S_{1:2}$	15	93.2
$S_{1:2}$	17	88.7
$S_{1:4}$	11	97.9
$S_{1:4}$	17	93.3
$S_{1:4}$	25	95.8

2.2.2. T-Shaped Indo Ring Arrangement Stabilizes CA/Indo Aggregates. Inspection of both the CA/Indo and pure-Indo clusters indicated that $\pi-\pi$ interaction is the primary reason for Indo's propensity to aggregate (Figure 5). This interaction is common among aromatic residues in proteins, where it plays an important structural role.[49−53] Similarly, Indo molecules in CA/Indo micelles (as well as in pure-Indo micelles) are held together by π interactions involving the chlorinated six-membered ring (A-ring) of Indo, which forms the core of the micelles. To quantify this observation, we used the distance (d) between the centroids and the angle (θ) between vectors perpendicular to the plane of the two A-rings of Indo. The d versus θ contour in Figure 6 shows that the majority of the stable Indo/CA micelles are characterized by $\theta \approx 90°$ and $d \approx 5-8$ Å. In fact, all of the most populated mixed micelles that contain 11−20 Indo molecules prefer such a perpendicular (T-shape) ring arrangement, especially at large separations (Figure 6). This is consistent with previous observations in aromatic−aromatic interactions in general[54] and poly aromatic surfactants in particular.[55] In addition, from a thermodynamic perspective, a T-shape arrangement can be energetically favorable because the alternative (stacked) arrangement would cause steric clashes involving the adjacent rings. Another advantage of T-shape arrangement is that it reduces the intra-Indo repulsion because of the negative charge. In addition to the inter-Indo interactions, the core of the mixed micelles was also stabilized by CA-Indo interactions. These interactions arise from the inherent amphipathicity of both species and require the packing of the hydrophobic β-face of CA with the chlorinated ring of Indo (Figure S8). The core of the micelle is dry, and the density of water increases toward the periphery, similar to that in CA/Ibu micelles.[37]

2.2.3. Structure of CA/Indo/POPC Micelles. We have seen in previous sections that CA/Indo form large mixed micelles primarily because of solvent exclusion followed by subsequent interactions involving the hydrophobic β-face of CA and the A-ring of Indo. The question is how POPC might alter these interactions. A closer look at the most stable CA/Indo/POPC ternary micelles listed in Table 3 indicates that the number of CA and Indo molecules within the ternary micelles does not follow any particular pattern, with either CA or Indo being disproportionately represented. Moreover, in each of these micelles, the core is made up of the acyl chain of POPC, as can be seen from the distribution of the POPC tail carbons relative to the peaks for the hydrophobic face of CA (CA:C18 at ∼18

dx.doi.org/10.1021/bi400723r | Biochemistry 2013, 52, 7461−7469

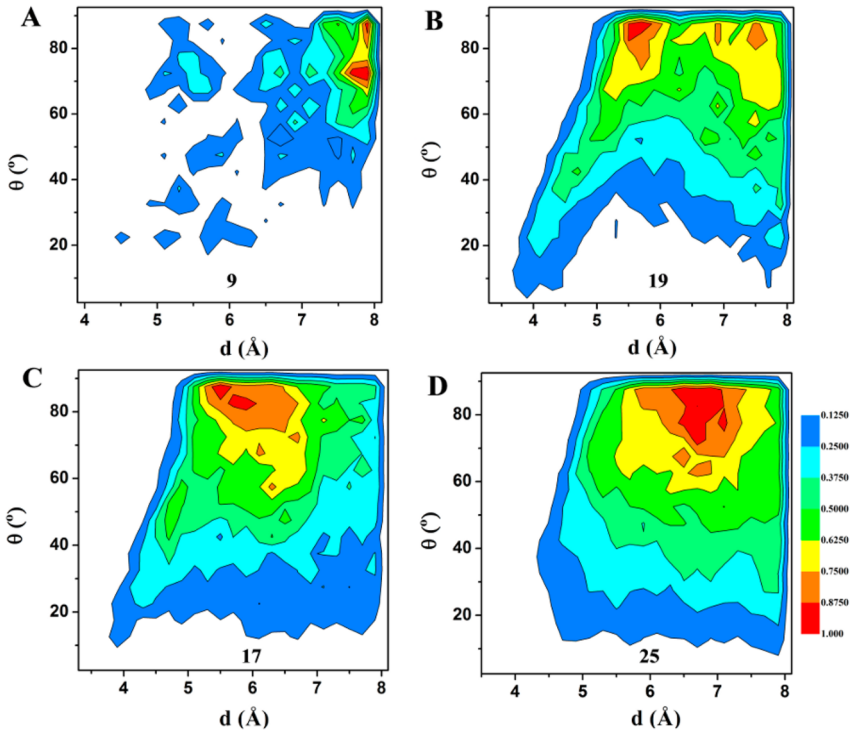

Figure 6. Intermolecular interactions among Indo molecules within CA/Indo mixed micelles. Two-dimensional distribution of the angle between the vector perpendicular to the planes of two chlorinated six-membered A-rings of Indo (θ) and the distance between the centroids of the A-rings (d). Shown here are averages over the last 10 ns of the data for the largest stable aggregate from simulation (A) $S_{1:0.5}$, (B) $S_{1:1}$, (C) $S_{1:2}$, and (D) $S_{1:4}$. Red denotes the most populated areas.

Table 3. Average Number of CA and Indo Molecules within Selected CA/Indo/POPC Ternary Micelles

simulation	aggregate size	no. of Indo	no. of CA
$S^{P}_{1:1}$	28	5	3
$S^{P}_{1:1}$	46	6	10
$S^{P\prime}_{1:1}$	31	10	6
$S^{P\prime}_{1:1}$	29	8	8
$S^{P}_{1:0.5}$	54	9	17
$S^{P}_{1:0.5}$	24	5	14

Å) and the hydrophobic tail of Indo (Indo:Cl at ∼15 Å). Although Indo inserts deeper than CA, both are localized near the rim of the mixed micelle (Figure 7). In fact, as seen in our previous study of CA/Ibu/DPC[37] as well as in other theoretical studies,[33,36,37] CA was found to lie parallel to the surface, with its hydrophobic face pointing toward the core. In contrast, Indo inserts its chlorinated six-membered ring about halfway to the center of the mixed micelle. The hydrophilic oxygen atoms of both Indo and CA were near the POPC headgroup (Figure 7).

2.2.4. POPC Attenuates Aggregation of CA with Indo. We assessed the aggregation of CA and Indo in the presence of POPC on the basis of N_N (Table 1), which was obtained using the same aggregate definition as in the case of the CA/Indo binary mixtures. Overall, one can see that N_N is dramatically smaller in the ternary than the binary mixtures, indicating perturbation of CA/Indo aggregation by POPC. This is because almost all of the CA and Indo molecules were distributed on the surface of the ternary micelles in a manner that minimized interaction among them. To quantify this observation, we looked at the distribution of CA and Indo in the ternary micelle by calculating the radial distance, r_d, between each pair of surface-bound (i) CA and every-other CA, (ii) Indo and every-other Indo, and (iii) CA and every-other Indo (Figure 8). For this analysis, we focused on the largest ternary micelle of size 54 from $S^{P}_{1:0.5}$ containing 17 CA and 9 Indo molecules. To calculate radial distances among CA pairs, the region around a given CA was binned into concentric circles separated by 1 Å, with the diameter of the outermost circle being greater than or equal to the diameter of the micelle in order to ensure the inclusion of every pair. This way, 16 of the 17 CA molecules would lie at a specific bin located a certain distance away from the (central) CA of interest. This was repeated 16 times (for each CA), and an average was taken. Similarly for each Indo/Indo and CA/Indo pair. An interesting result emerging from

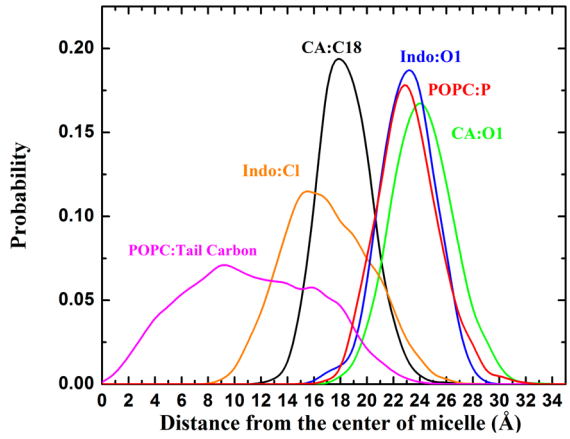

Figure 7. Probability distribution of specific atoms of POPC, CA, and Indo within a ternary mixed micelle of size 54 from simulation $S^{P}_{1:0.5}$. The last 30 ns of the trajectory was used for this analysis. Refer to Figure 1 for atom numbering.

dx.doi.org/10.1021/bi400723r | *Biochemistry* 2013, 52, 7461−7469

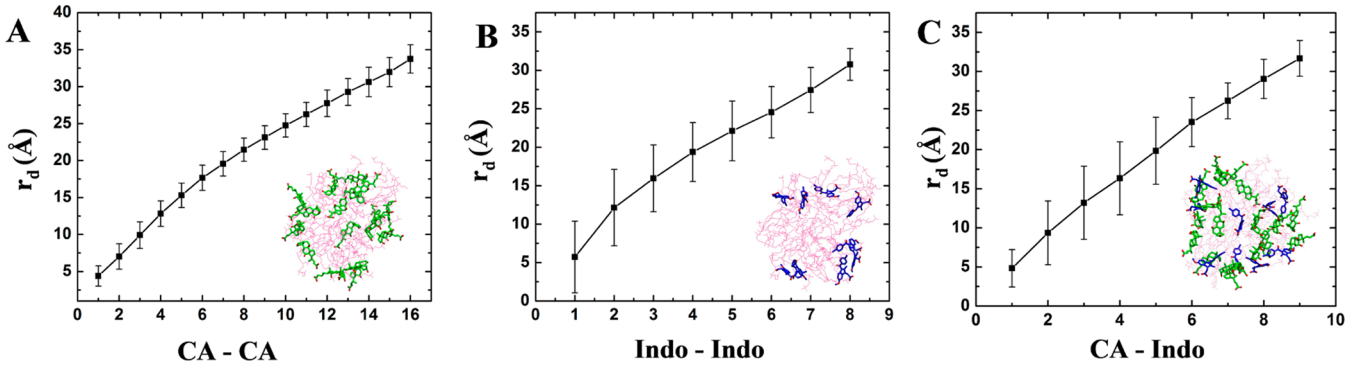

Figure 8. Distribution of CA and Indo in the CA/Indo/POPC ternary micelle. Radial distances (r_d) between (A) CA/CA pairs, (B) Indo/Indo pairs, and (C) Indo/CA pairs. Averages were taken over the last 10 ns of simulation $S^{P}_{1:0.5}$ and for an aggregate size of 54. Refer to Figures 3 or 5 for the color code. See the text for the description of these distances.

this analysis was that each CA molecule is located approximately 3 Å away from its nearest CA neighbor and 6 Å from the next nearest neighbor (Figure 8A). The approximately equal spacing between the neighbors indicates that CA molecules avoided each other and were uniformly distributed over the entire surface of the ternary micelle. Indo molecules adopted a somewhat similar distribution (Figure 8B), as did CA molecules relative to Indo (Figure 8C). No more than three Indo molecules reside within ~10 Å of another Indo (Figure 8B, inset) or are near a CA molecule (Figure 8C, inset). This distribution ensured that the maximum CA/Indo aggregate size does not exceed 5. We conclude that POPC acts as a dispersant that minimizes the formation of large pure-CA, pure-Indo, or CA/Indo micelles.

3. CONCLUSIONS

We have shown that CA and Indo binary mixtures spontaneously assemble into mixed micelles of variable sizes. Among the predominant aggregates, those of sizes 11 and 17 were obtained from two independent binary CA/Indo simulations with a higher Indo concentration, suggesting a nonrandom organization. Although the reactant with the higher relative concentration generally aggregates faster, increasing the Indo fraction resulted in the formation of stable, less dynamic, and relatively large binary mixed micelles. The halogenated ring of the Indo molecules within micelles adopted a T-shape arrangement that minimizes steric clashes among the adjacent rings. This arrangement exposes part of the Indo hydrophobic surface. The facially amphipathic CA molecules aggregate on the exposed hydrophobic surface of Indo aggregates. Significantly smaller CA/Indo aggregates were formed in the presence of POPC. This is because almost all of the CA and Indo molecules are involved in the formation of a CA/Indo/POPC ternary micelle wherein CA and Ibu distribute on the surface almost uniformly so that they are farther away from each other.

Experiments have shown a dose-dependent increase in the permeation of cell membranes by Indo in the presence of bile salts.[13,24] This effect was reduced by adding PCs.[13,56,57] In our simulations, increasingly larger and more stable CA/Indo aggregates were observed upon increasing the Indo fraction, and the presence of POPC diminished the interaction among CA and Indo and thereby prevented the formation of large CA/Indo aggregates. Taken together, these results suggest that large CA/Indo binary aggregates in the absence of POPC might be responsible for the observed toxicity of BA/Indo mixtures and the preventive action of PCs. We note that atomistic simulations are computationally expensive and binary/ternary mixtures take a long simulation time to fully equilibrate. Therefore, some of the quantitative aspects of the mixed micelles derived from the simulations should be interpreted with care. Nonetheless, the qualitative data clearly show that NSAIDs are able to aggregate with bile acids and that different NSAIDs form mixed micelles of varying sizes and morphology. Some of these NSAID-BA micelles may disrupt the mucosal membrane and hence become toxic, whereas PCs may mask this toxicity by minimizing NSAID-BA association.

■ ASSOCIATED CONTENT

Supporting Information

Time evolution of number-averaged aggregation numbers from CA/Indo, pure-Indo, and CA/Indo/POPC simulations; snapshot of a typical CA-Indo mixed micelle; size distribution of pure-CA micelles within a CA/POPC mixture; size distribution of CA/Indo micelles in a 4:1 mixture; bivariate distribution of the ratio of principal moments of inertia; and distribution of selected atoms within the largest ternary mixed micelle. This material is available free of charge via the Internet at http://pubs.acs.org.

■ AUTHOR INFORMATION

Corresponding Author

*Tel: 713-500-7538; E-mail: alemayehu.g.abebe@uth.tmc.edu.

Notes

The authors declare no competing financial interest.

■ ACKNOWLEDGMENTS

P.P. gratefully acknowledges a postdoctoral fellowship funded by the CPRIT Computational Cancer Biology Training Program (CCBTP) from the Cancer Prevention and Research Institute of Texas (CPRIT) (grant no. RP101489). We are thankful to the Texas Advanced Computing Center (TACC) for computational resources and Drs. Lenard Lichtenberger, Elizabeth Dial, and Yong Zhou for inspirational discussions. We thank Dr. Abdallah Sayyed-Ahmad for performing the initial POPC/CA simulations as well as members of the Gorfe laboratory for useful discussions.

■ ABBREVIATIONS USED

BA, bile acid; CA, cholic acid; Indo, indomethacin; DPC, dodecylphosphocholine; POPC, palmitoyloleylphosphatidylcholine; N_N number-averaged aggregation number

■ REFERENCES

(1) Dial, E. J., Darling, R. L., and Lichtenberger, L. M. (2008) Importance of biliary excretion of indomethacin in gastrointestinal and hepatic injury. *J. Gastroenterol. Hepatol. 23*, e384−e389.

(2) Petruzzelli, M., Vacca, M., Moschetta, A., Cinzia Sasso, R., Palasciano, G., Erpecum, K.J. van, and Portincasa, P. (2007) Intestinal mucosal damage caused by non-steroidal anti-inflammatory drugs: Role of bile salts. *Clin. Biochem. 40*, 503−510.

(3) Zhou, Y., Dial, E. J., Doyen, R., and Lichtenberger, L. M. (2010) Effect of indomethacin on bile acid-phospholipid interactions: implication for small intestinal injury induced by nonsteroidal anti-inflammatory drugs. *Am. J. Physiol.: Gastrointest. Liver Physiol. 298*, G722−731.

(4) Endo, H., Hosono, K., Inamori, M., Nozaki, Y., Yoneda, K., Fujita, K., Takahashi, H., Yoneda, M., Abe, Y., Kirikoshi, H., Kobayashi, N., Kubota, K., Saito, S., Ohya, T., Hisatomi, K., Teratani, T., Matsuhashi, N., and Nakajima, A. (2009) Characteristics of small bowel injury in symptomatic chronic low-dose aspirin users: the experience of two medical centers in capsule endoscopy. *J. Gastroenterol. 44*, 544−549.

(5) Goldstein, J. L., Eisen, G. M., Lewis, B., Gralnek, I. M., Zlotnick, S., and Fort, J. G. (2005) Video capsule endoscopy to prospectively assess small bowel injury with celecoxib, naproxen plus omeprazole, and placebo. *Clin. Gastroenterol. Hepatol. 3*, 133−141.

(6) Graham, D. Y., Opekun, A. R., Willingham, F. F., and Qureshi, W. A. (2005) Visible small-intestinal mucosal injury in chronic NSAID users. *Clin. Gastroenterol. Hepatol. 3*, 55−59.

(7) Cryer, B., and Kimmey, M. B. (1998) Gastrointestinal side effects of nonsteroidal anti-inflammatory drugs. *Am. J. Med. 105*, 20S−30S.

(8) Fortun, P. J., and Hawkey, C. J. (2007) Nonsteroidal antiinflammatory drugs and the small intestine. *Curr. Opin. Gastroenterol. 23*, 134−141.

(9) Singh, G., and Triadafilopoulos, G. (1999) Epidemiology of NSAID induced gastrointestinal complications. *J. Rheumatol., Suppl. 56*, 18−24.

(10) Flower, R., Gryglewski, R., Herbaczynska-Cedro, K., and Vane, J. R. (1972) Effects of anti-inflammatory drugs on prostaglandin biosynthesis. *Nat. New Biol. 238*, 104−106.

(11) Smith, J. B., and Willis, A. L. (1971) Aspirin selectively inhibits prostaglandin production in human platelets. *Nat. New Biol. 231*, 235−237.

(12) Lichtenberger, L. M. (2001) Where is the evidence that cyclooxygenase inhibition is the primary cause of nonsteroidal anti-inflammatory drug (NSAID)-induced gastrointestinal injury? Topical injury revisited. *Biochem. Pharmacol. 61*, 631−637.

(13) Petruzzelli, M., Moschetta, A., Renooij, W., De Smet, M., Palasciano, G., Portincasa, P., and Van Erpecum, K. (2006) Indomethacin enhances bile salt detergent activity: Relevance for NSAIDs-induced gastrointestinal mucosal injury. *Dig. Dis. Sci. 51*, 766−774.

(14) Tegeder, I., Pfeilschifter, J., and Geisslinger, G. (2001) Cyclooxygenase-independent actions of cyclooxygenase inhibitors. *FASEB J. 15*, 2057−2072.

(15) Duggan, D. E. (1975) Enterohepatic circulation of indomethacin and its role in intestinal irritation. *Biochem. Pharmacol. 24*, 1749−1754.

(16) Yamada, T. (1993) Mechanisms of acute and chronic intestinal inflammation induced by indomethacin. *Inflammation 17*, 641−662.

(17) Venneman, N. G., Petruzzelli, M., van Dijk, J. E., Verheem, A., Akkermans, L. M. A., Kroese, A. B. A., and van Erpecum, K. J. (2006) Indomethacin disrupts the protective effect of phosphatidylcholine against bile salt-induced ileal mucosa injury. *Eur. J. Clin. Invest. 36*, 105−112.

(18) Dial, E. J., Rooijakkers, S. H., Darling, R. L., Romero, J. J., and Lichtenberger, L. M. (2008) Role of phosphatidylcholine saturation in preventing bile salt toxicity to gastrointestinal epithelia and membranes. *J. Gastroenterol. Hepatol. 23*, 430−436.

(19) Lichtenberger, L. M., Barron, M., and Marathi, U. (2009) Association of phosphatidylcholine and nsaids as a novel strategy to reduce gastrointestinal toxicity. *Drugs Today 45*, 877−890.

(20) Cryer, B., Bhatt, D. L., Lanza, F. L., Dong, J. F., Lichtenberger, L. M., and Marathi, U. K. (2011) Low-dose aspirin-induced ulceration is attenuated by aspirin-phosphatidylcholine: A randomized clinical trial. *Am. J. Gastroenterol. 106*, 272−277.

(21) Anand, B. S., Romero, J. J., Sanduja, S. K., and Lichtenberger, L. M. (1999) Phospholipid association reduces the gastric mucosal toxicity of aspirin in human subjects. *Am. J. Gastroenterol. 94*, 1818−1822.

(22) Boggara, M. B., Faraone, A., and Krishnamoorti, R. (2010) Effect of pH and ibuprofen on the phospholipid bilayer bending modulus. *J. Phys. Chem. B 114*, 8061−8066.

(23) Boggara, M. B., and Krishnamoorti, R. (2009) Small-angle neutron scattering studies of phospholipid−NSAID adducts. *Langmuir 26*, 5734−5745.

(24) Lichtenberger, L. M., Zhou, Y., Dial, E. J., and Raphael, R. M. (2006) NSAID injury to the gastrointestinal tract: Evidence that NSAIDs interact with phospholipids to weaken the hydrophobic surface barrier and induce the formation of unstable pores in membranes. *J. Pharm. Pharmacol. 58*, 1421−1428.

(25) Hofmann, A. F. (1999) Bile Acids: The good, the bad, and the ugly. *News Physiol. Sci. 14*, 24−29.

(26) Hofmann, A. F., and Mysels, K. J. (1988) Bile salts as biological surfactants. *Colloids Surf. 30*, 145−173.

(27) Monte, M. J., Antelo, A., and Vazquez-Tato, J. (2009) Bile acids: Chemistry, physiology, and pathophysiology. *World J. Gastroenterol. 21*, 804−816.

(28) Barrios, J. M., and Lichtenberger, L. M. (2000) Role of biliary phosphatidylcholine in bile acid protection and NSAID injury of the ileal mucosa in rats. *Gastroenterology 11*, 1179−1186.

(29) Warren, D. B., Chalmers, D. K., Hutchison, K., Dang, W., and Pouton, C. W. (2006) Molecular dynamics simulation of spontaneous bile salt aggregation. *Colloids Surf., A 280*, 182−193.

(30) Verde, A. V., and Frenkel, D. (2010) Simulation study of micelle formation by bile salts. *Soft Matter 6*, 3815−3825.

(31) Carey, M. C., and Small, D. M. (1972) Micelle formation by bile salts: Physical-chemical and thermodynamic considerations. *Arch. Intern. Med. 130*, 506−527.

(32) Pártay, L. B., Jedlovszky, P., and Sega, M. (2007) Molecular aggregates in aqueous solutions of bile acid salts. Molecular dynamics simulation study. *J. Phys. Chem. B 111*, 9886−9896.

(33) Sayyed-Ahmad, A., Lichtenberger, L. M., and Gorfe, A. A. (2010) Structure and dynamics of cholic acid and dodecylphosphocholine−cholic acid aggregates. *Langmuir 26*, 13407−13414.

(34) Nichols, J. W., and Ozarowski, J. (1990) Sizing of lecithin-bile salt mixed micelles by size-exclusion high-performance liquid chromatography. *Biochemistry 29*, 4600−4606.

(35) Pártay, L. B., Sega, M., and Jedlovszky, P. (2007) Morphology of bile salt micelles as studied by computer simulation methods. *Langmuir 23*, 12322−12328.

(36) Marrink, S. J., and Mark, A. E. (2002) Molecular dynamics simulations of mixed micelles modeling human bile. *Biochemistry 41*, 5375−5382.

(37) Prakash, P., Sayyed-Ahmad, A., Zhou, Y., Volk, D. E., Gorenstein, D. G., Dial, E., Lichtenberger, L. M., and Gorfe, A. A. (2012) Aggregation behavior of ibuprofen, cholic acid and dodecylphosphocholine micelles. *Biochim. Biophys. Acta 1818*, 3040−3047.

(38) Mazer, N. A., Benedek, G. B., and Carey, M. C. (1980) Quasielastic light-scattering studies of aqueous biliary lipid systems. Mixed micelle formation in bile salt-lecithin solutions. *Biochemistry 19*, 601−615.

(39) Mazer, N. A., Carey, M. C., Kwasnick, R. F., and Benedek, G. B. (1979) Quasielastic light scattering studies of aqueous biliary lipid systems. Size, shape, and thermodynamics of bile salt micelles. *Biochemistry 18*, 3064−3075.
(40) Singh, J., Unlu, Z., Ranganathan, R., and Griffiths, P. (2008) Aggregate properties of sodium deoxycholate and dimyristoylphosphatidylcholine mixed micelles. *J. Phys. Chem. B 112*, 3997−4008.
(41) Ulmius, J., Lindblom, G., Wennerstrom, H., Johansson, L. B., Fontell, K., Soderman, O., and Arvidson, G. (1982) Molecular organization in the liquid−crystalline phases of lecithin−sodium cholate−water systems studied by nuclear magnetic resonance. *Biochemistry 21*, 1553−1560.
(42) Long, M. A., Kaler, E. W., and Lee, S. P. (1994) Structural characterization of the micelle-vesicle transition in lecithin-bile salt solution. *Biophys. J. 67*, 1733−1742.
(43) Hjelm, R. P., Thiyagarajan, P., and Alkan-Onyuksel, H. (1992) Organization of phosphatidylcholine and bile salt in rodlike mixed micelles. *J. Phys. Chem. 96*, 8653−8661.
(44) Coello, A., Meijide, F., Rodriguez Nunez, E., and Vazquez Tato, J. (1993) Aggregation behavior of sodium cholate in aqueous solution. *J. Phys. Chem. 97*, 10186−10191.
(45) Vanommeslaeghe, K., Hatcher, E., Acharya, C., Kundu, S., Zhong, S., Shim, J., Darian, E., Guvench, O., Lopes, P., Vorobyov, I., and Mackerell, A. D. (2010) CHARMM general force field: A force field for drug-like molecules compatible with the CHARMM all-atom additive biological force fields. *J. Comput. Chem. 31*, 671−690.
(46) MacKerell, A. D., Bashford, D., Bellot, M., Dunbrack, R. L., Evanseck, J. D., Field, M. J., Fischer, S., Gao, J., Guo, H., Ha, S., Joseph-McCarthy, D., Kuchnir, L., Kuczera, K., Mattos, F. T. K., Mattos, C., Michnick, S., Ngo, T., Nguyen, D. T., Prodhom, B., Reiher, W. E., Roux, B., Schlenkrich, M., Smith, J. C., Stote, R., Straub, J., Watanabe, M., Wiorkiewicz-Kuczera, J., Yin, D., and Karplus, M. (1998) All atom empirical potential for molecular modeling and dynamics studies of proteins. *J. Phys. Chem. B 102*, 3586−3616.
(47) Phillips, J. C., Braun, R., Wang, W., Gumbart, J., Tajkhorshid, E., Villa, E., Chipot, C., Skeel, R. D., Kalé, L., and Schulten, K. (2005) Scalable molecular dynamics with NAMD. *J. Comput. Chem. 26*, 1781−1802.
(48) Darden, T., York, D., and Pedersen, L. (1993) Particle mesh Ewald: An $N\cdot\log(N)$ method for Ewald sums in large systems. *J. Chem. Phys. 98*, 10089−10092.
(49) Waters, M. L. (2002) Aromatic interactions in model systems. *Curr. Opin. Chem. Biol. 6*, 736−741.
(50) Hunter, C. A., Singh, J., and Thornton, J. M. (1991) Pi-pi interactions: The geometry and energetics of phenylalanine-phenylalanine interactions in proteins. *J. Mol. Biol. 218*, 837−846.
(51) Anjana, R., Vaishnavi, M. K., Sherlin, D., Kumar, S. P., Naveen, K., Kanth, P. S., and Sekar, K. (2012) Aromatic-aromatic interactions in structures of proteins and protein-DNA complexes: A study based on orientation and distance. *Bioinformation 8*, 1220−1224.
(52) Gonzalez-Gutierrez, G., and Grosman, C. (2010) Bridging the gap between structural models of nicotinic receptor superfamily ion channels and their corresponding functional states. *J. Mol. Biol. 403*, 693−705.
(53) Ghosh, D., Kosenkov, D., Vanovschi, V., Williams, C. F., Herbert, J. M., Gordon, M. S., Schmidt, M. W., Slipchenko, L. V., and Krylov, A. I. (2010) Noncovalent interactions in extended systems described by the effective fragment potential method: Theory and application to nucleobase oligomers. *J. Phys. Chem. A 114*, 12739−12754.
(54) Chelli, R., Gervasio, F. L., Procacci, P., and Schettino, V. (2002) Stacking and T-shape competition in aromatic−aromatic amino acid interactions. *J. Am. Chem. Soc. 124*, 6133−6143.
(55) Teklebrhan, R. B., Ge, L., Bhattacharjee, S., Xu, Z., and Sjöblom, J. (2012) Probing structure−nanoaggregation relations of polyaromatic surfactants: A molecular dynamics simulation and dynamic light scattering study. *J. Phys. Chem. B 116*, 5907−5918.
(56) Lanza, F. L., Marathi, U. K., Anand, B. S., and Lichtenberger, L. M. (2008) Clinical trial: Comparison of ibuprofen-phosphatidylcholine and ibuprofen on the gastrointestinal safety and analgesic efficacy in osteoarthritic patients. *Aliment. Pharmacol. Ther. 28*, 431−442.
(57) Lichtenberger, L. M., Wang, Z. M., Romero, J. J., Ulloa, C., Perez, J. C., Giraud, M. N., and Barreto, J. C. (1995) Non-steroidal anti-inflammatory drugs (NSAIDs) associate with zwitterionic phospholipids: Insight into the mechanism and reversal of NSAID-induced gastrointestinal injury. *Nat. Med. 1*, 154−158.